

Supporting Information

Controllable Synthesis of Ultrasmall Pd Nanocatalyst Templated by Supramolecular Coordination Cage for Highly Efficient Reductive Dehalogenation

Wei-Ling Jiang,^a Ji-Chuang Shen,^a Zhiyong Peng,^a Guiyuan Wu,^a Guang-Qiang Yin,^b Xueliang Shi,^{*a} and Hai-Bo Yang^a

a Shanghai Key Laboratory of Green Chemistry and Chemical Processes, Chang-Kung Chuang, Institute, School of Chemistry and Molecular Engineering, East China Normal University, Shanghai 200062, P. R. China.

b Department of Chemistry, University of South Florida, Tampa, Florida 33620, United States

E-mail: xlshi@chem.ecnu.edu.cn

Table of Contents

1. Experimental section	2
1.1. General	2
1.2. Synthetic scheme and characterization data of four cages	3
2. General procedure for preparation of cage@CMC and Pd nanocatalysts	4
2.1. Preparation of cage@CMC- impregnation procedure	4
2.2. Preparation of Pd nanocatalysts-reduction procedure	5
3. Additional data for characterization of cage@CMC and Pd nanocatalysts	5
4. Catalytic studies	11
4.1. General procedure for dechlorination reaction.....	11
4.2. Continuous flow reactor for degradation of PCB 77	11
4.3. Recycling of the catalyst.....	12

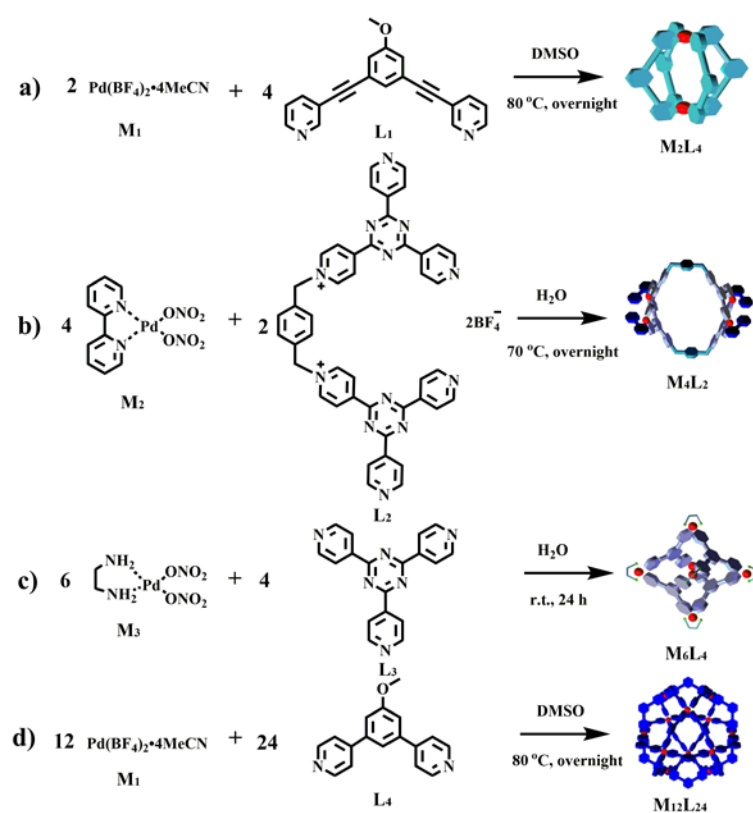
1. Experimental section

1.1. General

All chemicals were purchased from commercial sources and used without further purification. All solvents were analytical grade and distilled prior to use. Powder X-ray diffraction pattern of samples was determined using a Rigaku RU-200b with Cu K α radiation ($\lambda = 1.5406 \text{ \AA}$). Solution ^1H NMR spectra were recorded on Bruker 500 MHz Spectrometer at 298 K. Solid ^{13}C NMR spectra were collected on Agilent 600 MHz NMR spectrometer. Electrospray ionization (ESI) mass spectra were recorded with a Waters Synapt G2 mass spectrometer. Infrared (IR) spectra were obtained using a Bruker tensor 27 infrared spectrometer. Thermogravimetric analysis (TGA) was performed on a Netzsch STA 449 F3 instrument. The sample was heated from room temperature to 1073 K with the heating rate of $10 \text{ K}\cdot\text{min}^{-1}$ under a flow of nitrogen ($10 \text{ mL}\cdot\text{min}^{-1}$). Scanning electron microscopy (SEM) images of the solutions were obtained using an S-4800 (Hitachi Ltd.) with an accelerating voltage of 3.0-10.0 kV. Transmission electron microscopy (TEM) images were recorded on a Tecnai G2 F30 (FEI Ltd.) at 300 kV. The samples were dripped on a Holey carbon coated TEM-grid (300 mesh Cu grid, Pacific Grid Tech, USA) after being dispersed in ethanol by ultrasound. The amounts of palladium in the composites were measured by inductively coupled plasma atomic emission spectrometer (ICP-AES). Elemental analysis was carried out on an PE (PerkinElmer) EA2400 II elemental analyzer. XPS spectra were recorded on a Thermo Fisher ESCALAB 250Xi system with Al K α radiation, operated at 150 W. The identification and quantitation of products were performed on a gas chromatograph-mass spectrometer (GC-MS) (SHIMADZU GCMSQP2020 equipped with a $0.25 \text{ mm} \times 30 \text{ m}$ Rtx-5MS capillary column).

1.2. Synthetic scheme and characterization data of four cages

Ligand **L**₁, **L**₂, **L**₃, **L**₄, and cages **M**₄**L**₂ and **M**₆**L**₄ were prepared according to the literatures.^{S1-S6}



Scheme S1. The synthetic route to the four supramolecular coordination cages.

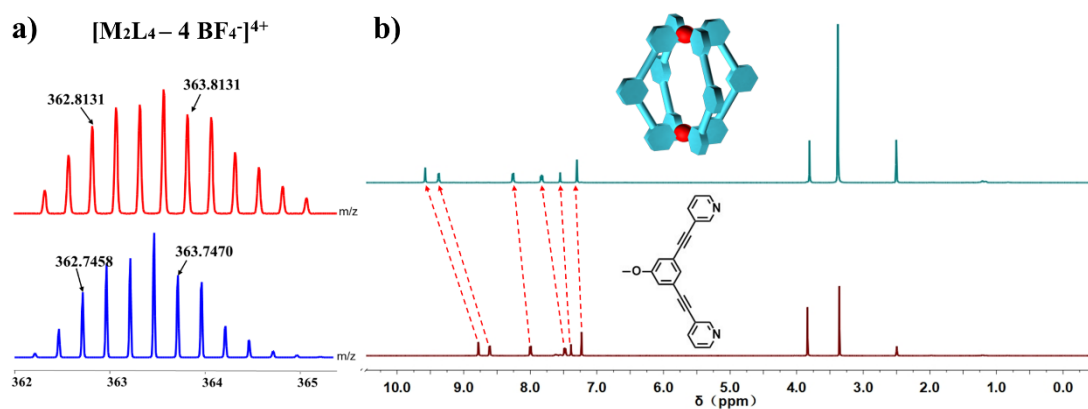


Figure S1. (a) The ESI-MS and isotopic pattern of cage **M**₂**L**₄. (b) The ¹H NMR spectra (500 MHz, DMSO-*d*₆, 298 K) of 120° pyridine ligand **L**₁ (bottom) and cage **M**₂**L**₄ (top).

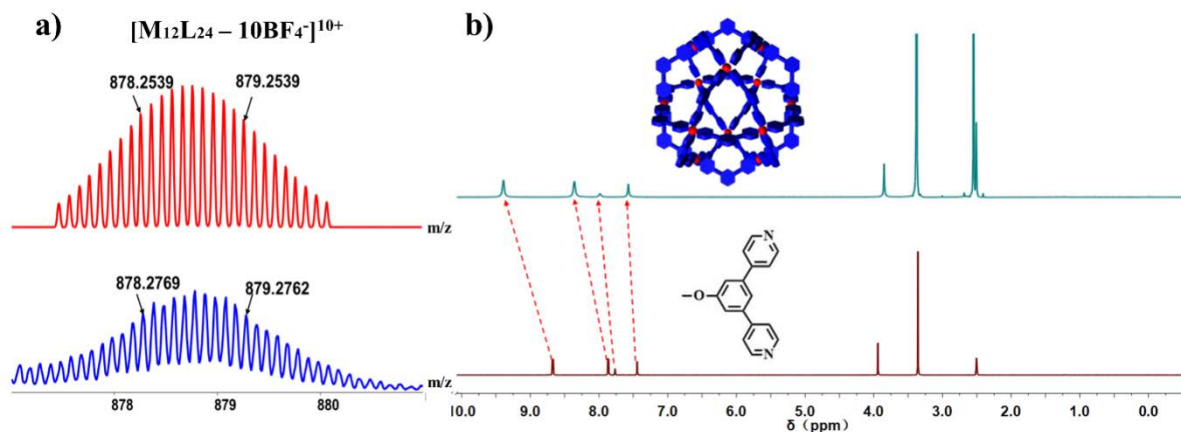


Figure S2. (a) The ESI-MS and isotopic pattern of cage $M_{12}L_{24}$. (b) The 1H NMR spectra (500 MHz, $DMSO-d_6$, 298 K) of 120° pyridine ligand L_2 (bottom) and cage $M_{12}L_{24}$ (top).

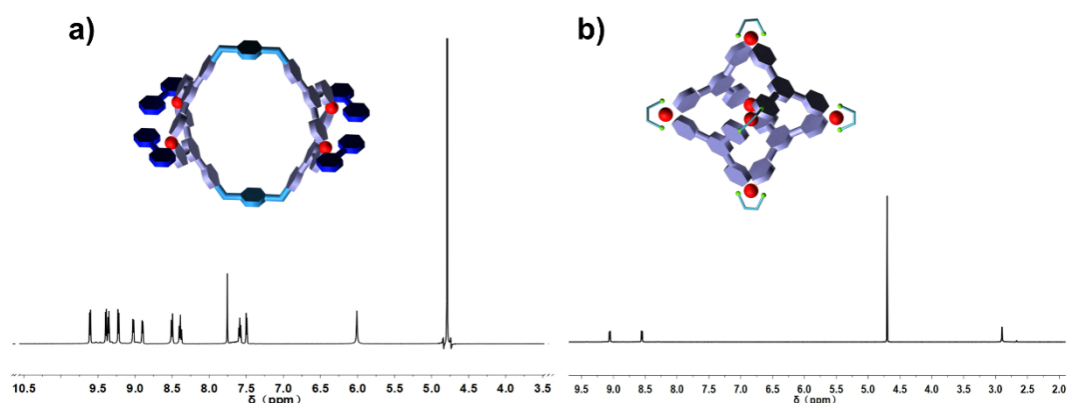


Figure S3. The 1H NMR spectra (500 MHz, D_2O , 298 K) of (a) cage M_4L_2 and (b) cage M_6L_4 .

2. General procedure for preparation of cage@CMC and Pd nanocatalysts

2.1. Preparation of cage@CMC- impregnation procedure

Dried powder of cage was dispersed in aqueous solution with sonication for 30 min in a 50 mL round-bottom flask, CMC was then added to the mixture with rapid agitation by mechanical agitation (1,000 rpm) for 5 h. After that the mixture was slowly transformed to sol, and then was poured into a cylindrical mold (3 cm in diameter and 3 cm in depth) made from PTFE (poly tetra fluoroethylene). Then the sol was soaked in acetonitrile solution until the sol was completely transformed into a gel. The obtained gel was then pre-frozen at $-19^\circ C$ overnight and freeze-dried under vacuum for 48 h, resulting in the cylinder-shape aerogel.

$M_2L_4@CMC$, $M_4L_2@CMC$, $M_6L_4@CMC$ and $M_{12}L_{24}@CMC$ were prepared by the above impregnation method.

2.2. Preparation of Pd nanocatalysts-reduction procedure

Pd nanocatalyst was obtained by soaking the corresponding cylinder-shape aerogel cage@CMC into freshly prepared methanol solution of $NaBH_4$. The mixture was stirring for 30 minutes, then washed by methanol for three times. The prepared Pd nanocatalyst was then dried under vacuum for 12 h.

$M_2@CMC$, $M_4@CMC$, $M_6@CMC$ and $M_{12}@CMC$ were prepared by the above reduction method.

3. Additional data for characterization of cage@CMC and Pd nanocatalysts

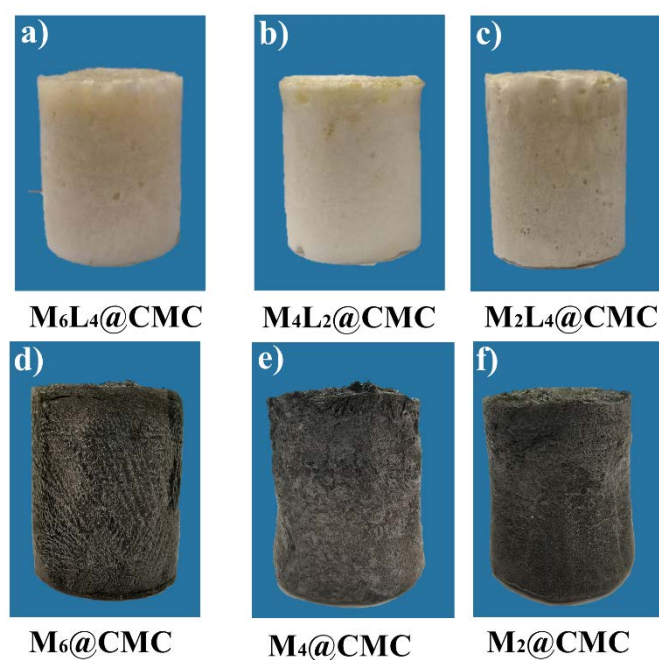


Figure S4. The photos of aerogels before and after reduction: (a) $M_6L_4@CMC$, (b) $M_4L_2@CMC$, (c) $M_2L_4@CMC$, (d) $M_6@CMC$, (e) $M_4@CMC$ and (f) $M_2@CMC$.

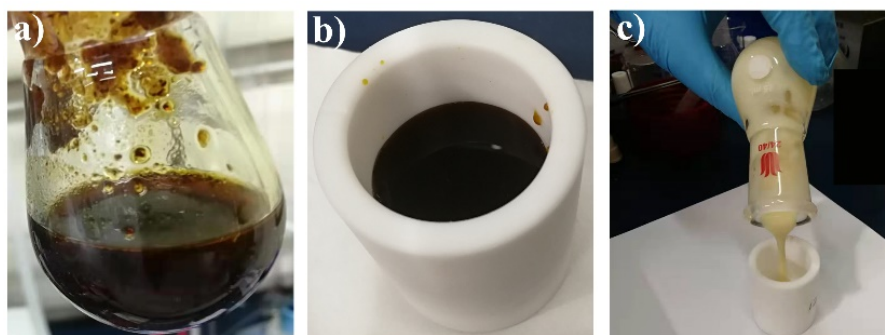


Figure S5. The photos of the mixture of (a and b) $\text{Pd}(\text{MeCN})_4(\text{BF}_4)_2$ and CMC and (c) the mixture of $\text{M}_{12}\text{L}_{24}@\text{CMC}$. The dark precipitate (a and b) indicated that $\text{M}_1@\text{CMC}$ cannot form aerogel, in contrast to the homogeneous fluid of $\text{M}_{12}\text{L}_{24}@\text{CMC}$ which could form the aerogel.

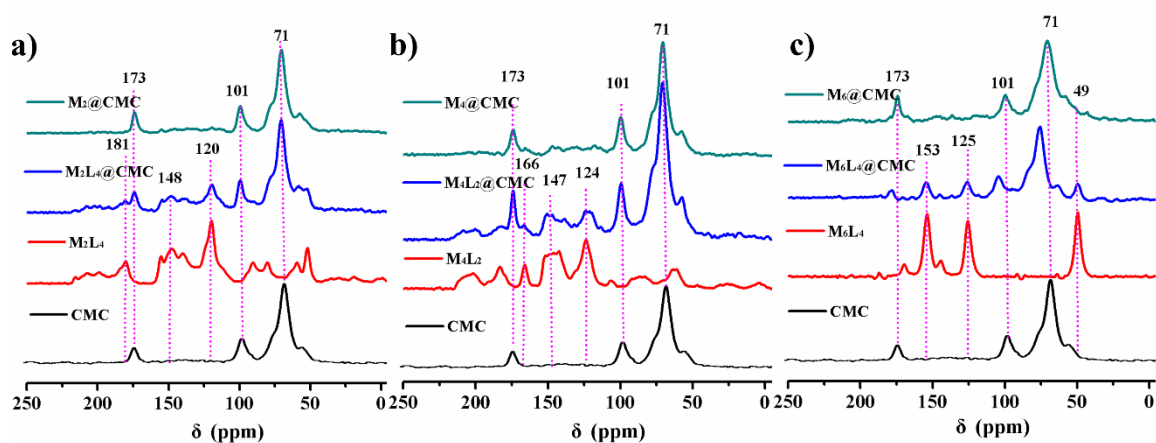


Figure S6. Stacked solid-state ^{13}C NMR spectra of (a) CMC (black), cage M_2L_4 (red), $\text{M}_2\text{L}_4@\text{CMC}$ (blue) and $\text{M}_2@\text{CMC}$ (green), (b) CMC (black), cage M_4L_2 (red), $\text{M}_4\text{L}_2@\text{CMC}$ (blue) and $\text{M}_4@\text{CMC}$ (green), and (c) CMC (black), cage M_6L_4 (red), $\text{M}_6\text{L}_4@\text{CMC}$ (blue) and $\text{M}_6@\text{CMC}$ (green).

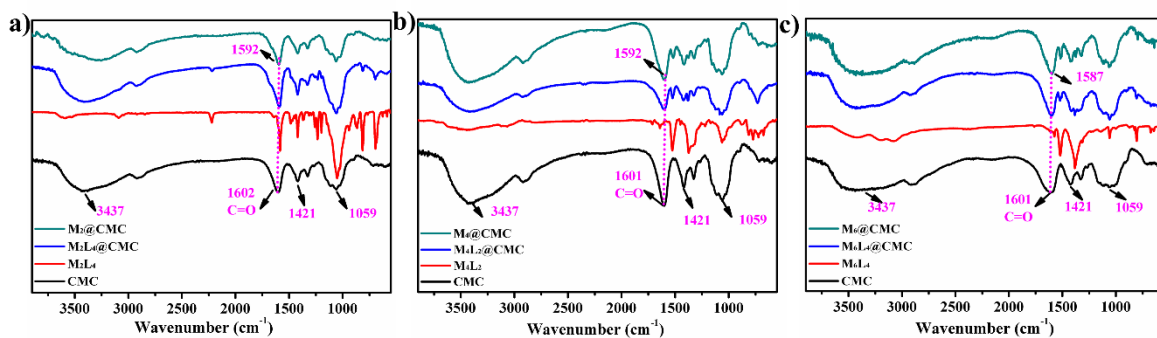


Figure S7. Stacked FT-IR spectra of (a) CMC (black), cage M_2L_4 (red), $M_2L_4@CMC$ (blue) and $M_2@CMC$ (green), (b) CMC (black), cage M_4L_2 (red), $M_4L_2@CMC$ (blue) and $M_4@CMC$ (green), and (c) CMC (black), cage M_6L_4 (red), $M_6L_4@CMC$ (blue) and $M_6@CMC$ (green).

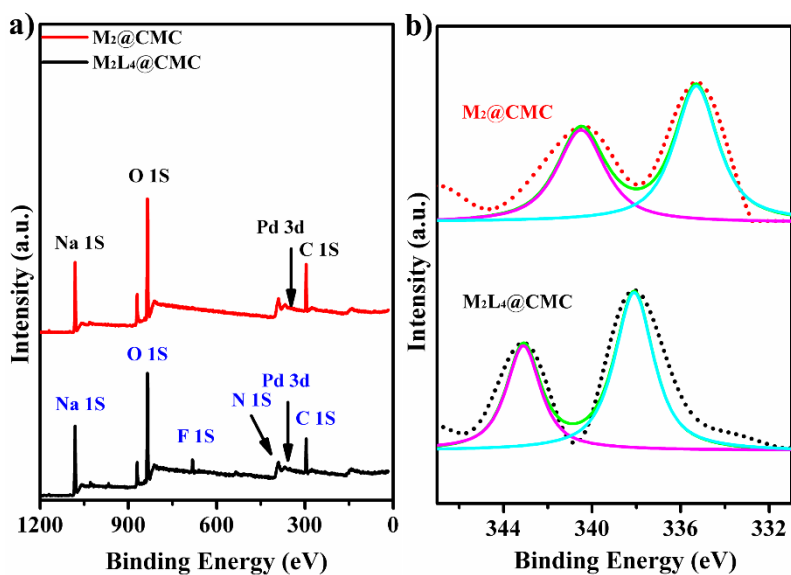


Figure S8. XPS spectra of $M_2L_4@CMC$ and $M_2@CMC$: (a) survey spectra, (b) high-resolution signals of Pd 3d.

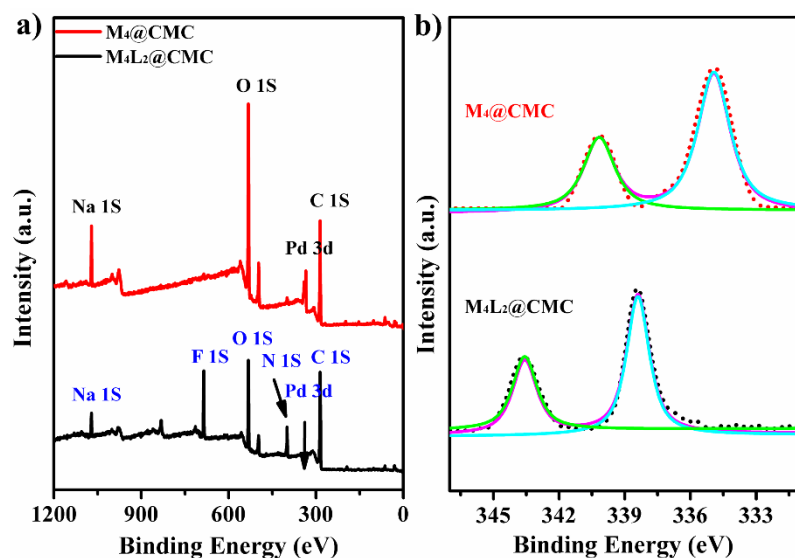


Figure S9. XPS spectra of $M_4L_2@CMC$ and $M_4@CMC$: (a) survey spectra, (b) high-resolution signals of Pd 3d.

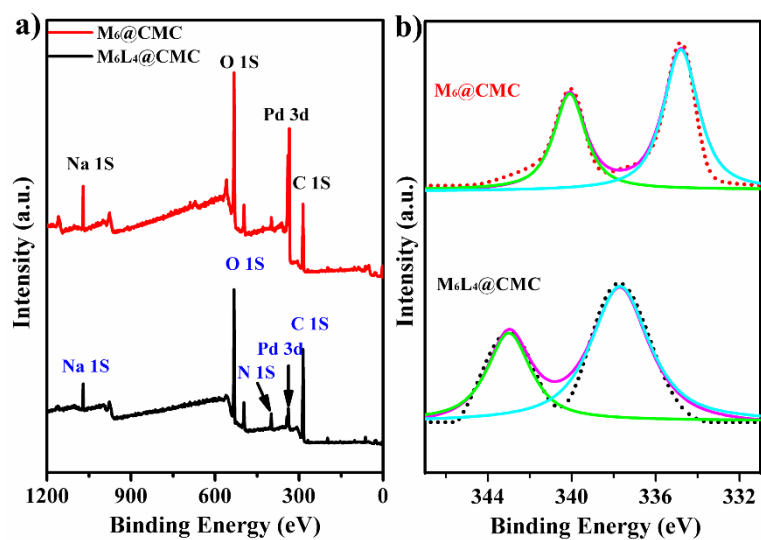


Figure S10. XPS spectra of $M_6L_4@CMC$ and $M_6@CMC$: (a) survey spectra, (b) high-resolution signals of Pd 3d.

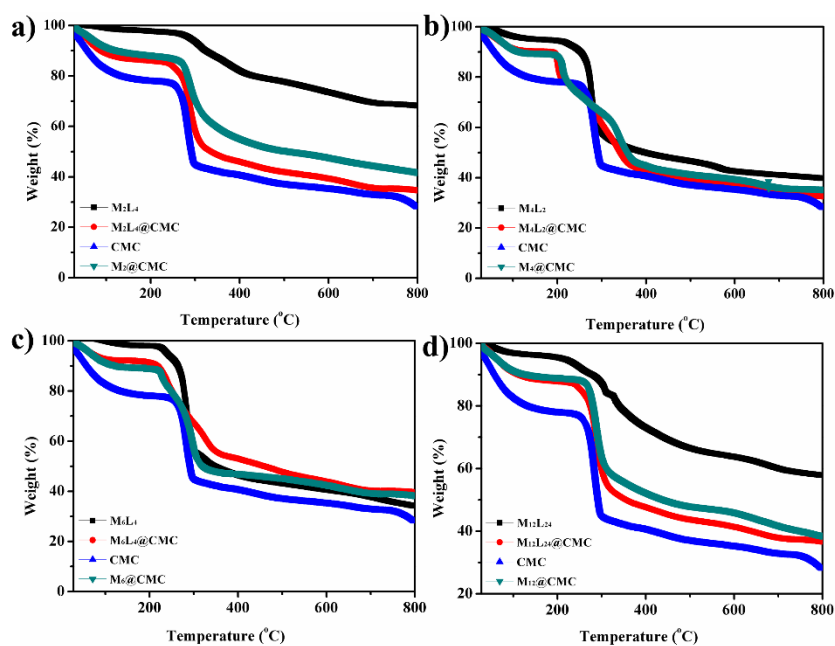


Figure S11. Stacked TGA spectra of (a) CMC, cage M_2L_4 , $M_2L_4@CMC$ and $M_2@CMC$, (b) CMC, cage M_4L_2 , $M_4L_2@CMC$ and $M_4@CMC$, (c) CMC, cage M_6L_4 , $M_6L_4@CMC$ and $M_6@CMC$, and (d) CMC, cage $M_{12}L_{24}$, $M_{12}L_{24}@CMC$ and $M_{12}@CMC$.

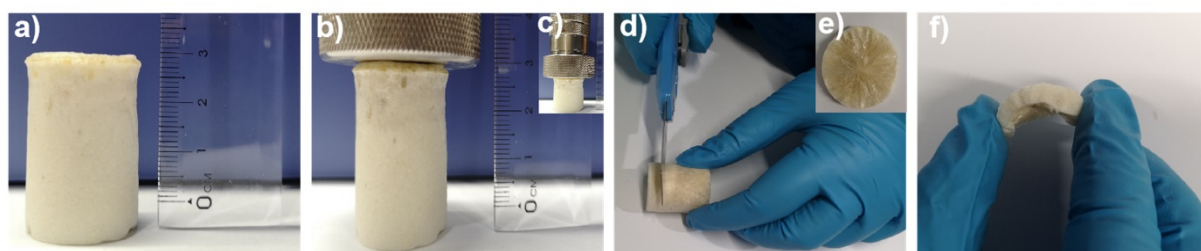


Figure S12. The mechanical test of the aerogel: (a,b,c) pressing experiment of the aerogel conducted with a 500 g autoclave, (d,e) the aerogel was cut into thin films with a knife, and (f) the obtained film exhibited a certain bending tolerance.

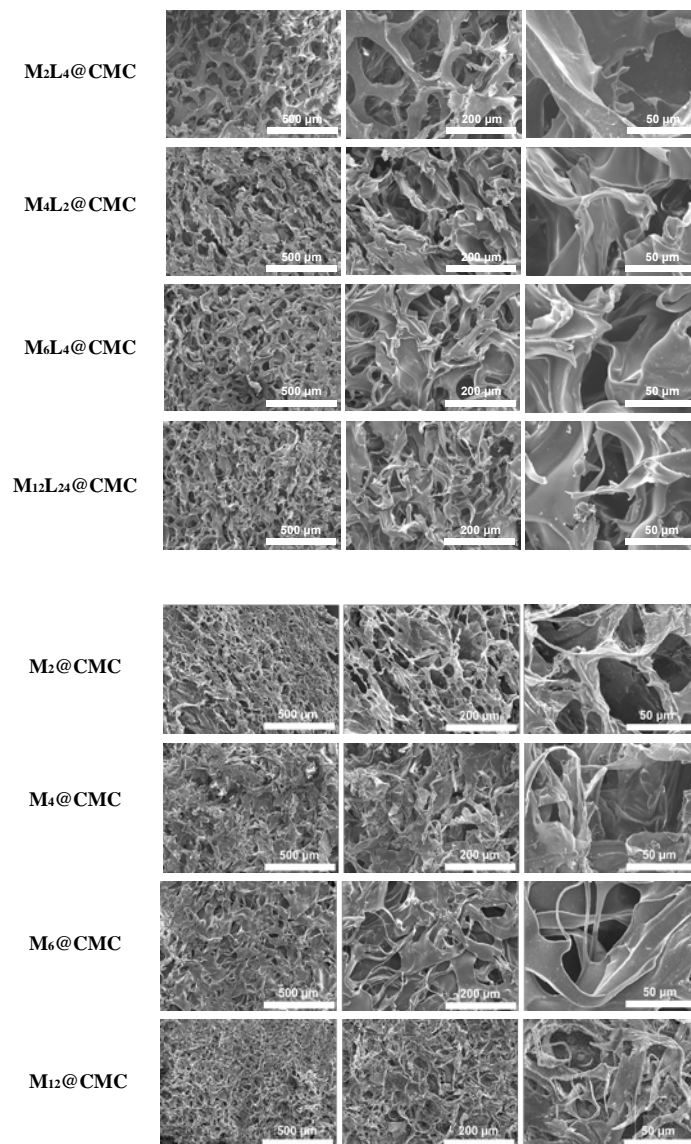


Figure S13. SEM images of the aerogel before and after reduction.

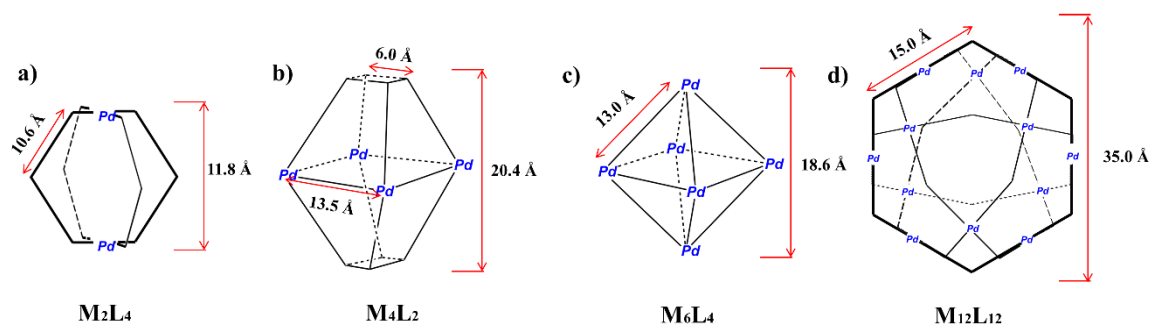


Figure S14. The estimated size of the four cages: (a) M_{2L4} , (b) M_{4L2} , (c) M_{6L4} , and (d) M_{12L24} .

Table S1. Original ICP results for the foam composites doped with different cages after reduction.

Entry	Pd Concentration	Volume (mL)	Sample Quality	Pd Content
3.5%- M₂@CMC	16.13	25	11.26	3.58
3.5%- M₄@CMC	17.47	25	12.47	3.50
3.5%- M₆@CMC	14.52	25	11.06	3.28
3.5%- M₁₂@CMC	9.49	25	6.72	3.53
0.1%- M₁₂@CMC	1.42	250	4.02	0.09
1.0%- M₁₂@CMC	5.65	25	13.10	1.07
5.0%- M₁₂@CMC	14.36	25	7.58	4.73
12.0%- M₁₂@CMC	33.39	25	6.61	12.63
12.0%- M₁₂@CMC 5 th -run	29.60	25	5.90	12.54

Sample treatment details: the aerogel sample was ground into a powder and then dried in a vacuum oven at 100 °C for 24 h. The above powder was digested with nitric acid and sulfuric acid, and then configured into an aqueous solution for testing.

4. Catalytic studies

4.1. General procedure for dechlorination reaction

The chlorinated substrate (0.05 mmol), ammonium formate (63 mg, 1.0 mmol) and 12 wt%-**M₁₂@CMC** (calculating according to 5 mol% of Pd) were added to a vessel with a mixed solvent of methanol (4 mL) and methanol/N, N-dimethyl formamide (4 mL, V/V, 1:1). Then the mixture was stirred at room temperature for several hours. The above reaction liquid was subsequently taken in the GC-MS test.

4.2. Continuous flow reactor for degradation of PCB 77

The reactor was designed based on a short Teflon column filled with the aerogel of **M₁₂@CMC**, and the figure of the setup and process was shown in Figure S23. In the continuous flow experiment, the solution of PCB 77 (150 mg, 0.5 mmol) and ammonium formate (630 mg, 10 mmol) in methanol/N, N-dimethyl formamide (V/V, 1:1) was continually pumped through reaction column using a peristaltic pump with a flow rate of 1 mL/min. The reaction system was periodically detected by *in situ* GC-MS analysis.

4.3. Recycling of the catalyst

The recyclability of the Pd nanocatalyst was tested under the general dechlorination reaction as described above using the 4-chloroaniline as a chlorinated substrate. For recycling of the catalyst, the catalyst of **M₁₂@CMC** was separated from the reaction mixture by filtration and washed three times by soaking in methanol at room temperature, separated by filtration and dried at 80 °C before each recycle run.

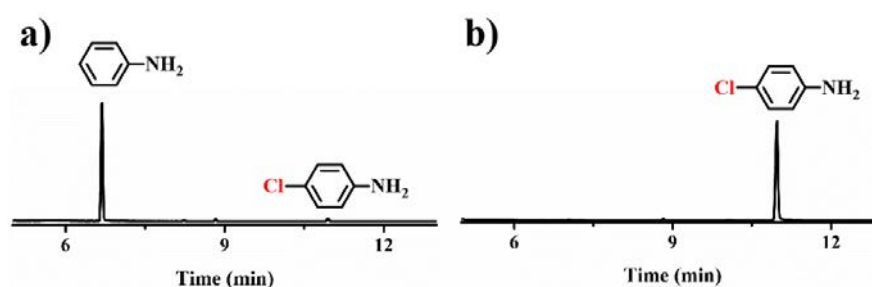
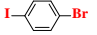
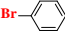
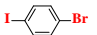

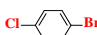
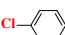
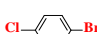
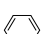


Figure S15. Gas chromatography (GC) analysis of the dechlorination of 4-chloroaniline (a) with and (b) without ammonium formate at room temperature.

Table S2. Dehalogenation of the substrates containing two different halogen atoms.

Entry	Substrate	Product	T (h)	Conversion (%)	Carbon balance (%)
1			5	99	98
2			11	98	97
3			6	98	98
4			16	99	98

Reaction conditions: chlorinated substrate (0.05 mmol), catalyst (calculating according to 5 mol% of Pd), ammonium formate (1 mmol) and methanol (4 ml) at room temperature. Conversion determined by GC-MS.

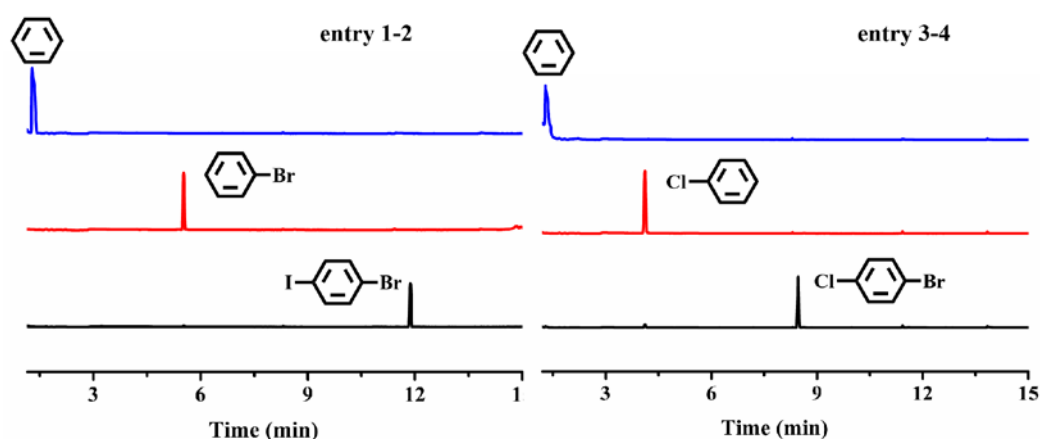


Figure S16. Gas chromatography (GC) analysis of the dehalogenation reaction in Table S2.

Table S3. The carbon balance value of the dechlorination reaction by **M₁₂@CMC**.

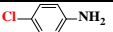
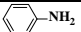
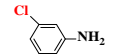
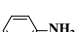

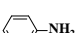
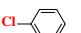
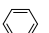
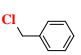

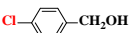
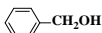


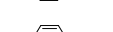

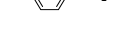
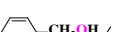
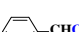



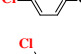
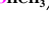
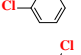
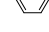
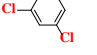
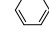
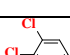
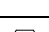
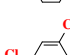

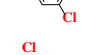

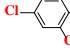
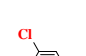
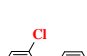

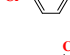
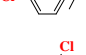
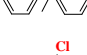


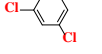

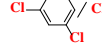
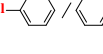
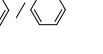
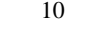
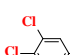
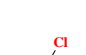
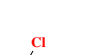

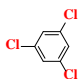
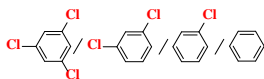
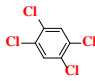
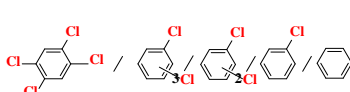
Entry	Substrate	Product	T (h)	Carbon balance (%)
1			6	98
2			6	98
3			6	95
4			5	99
5			1	99
6			6	98
7			6	99
8			5	99
9		 / 	3	98
10		 / 	22	97
11			10	98
12			10	98
13			15	98

Table S4. Summary of the dechlorination of the multiple chlorinated substrates in a mixed solvent system.

Entry	Substrate	Product	T (h)	Conversion (%)	Carbon balance (%)
1 ^a			10	99	98
2 ^a			10	99	98
3 ^a			15	99	98
4 ^b		 /  / 	10	95/1/1	98
5 ^b		 /  /  / 	10	86/4/5/2	98
6 ^b		 /  /  /  / 	15	60/8/18/9/3	98
7 ^c		 /  / 	10	88/5/4	97

8 ^c			10	64/9/15/9	97
9 ^c			15	22/6/16/24/31	98

Reaction conditions: chlorinated substrate (0.05 mmol), catalyst (calculating according to 5 mol% of Pd), ammonium formate (1 mmol), solvent (4 ml) at room temperature. ^aThe reaction was conducted in a mixed solvent of methanol and N, N-dimethyl formamide (V/V, 1:1). ^bThe reaction was conducted in a mixed solvent of methanol and tetrahydrofuran (V/V, 1:1). ^cThe reaction was conducted in mixed solvent of methanol and ethyl acetate (V/V, 1:1).

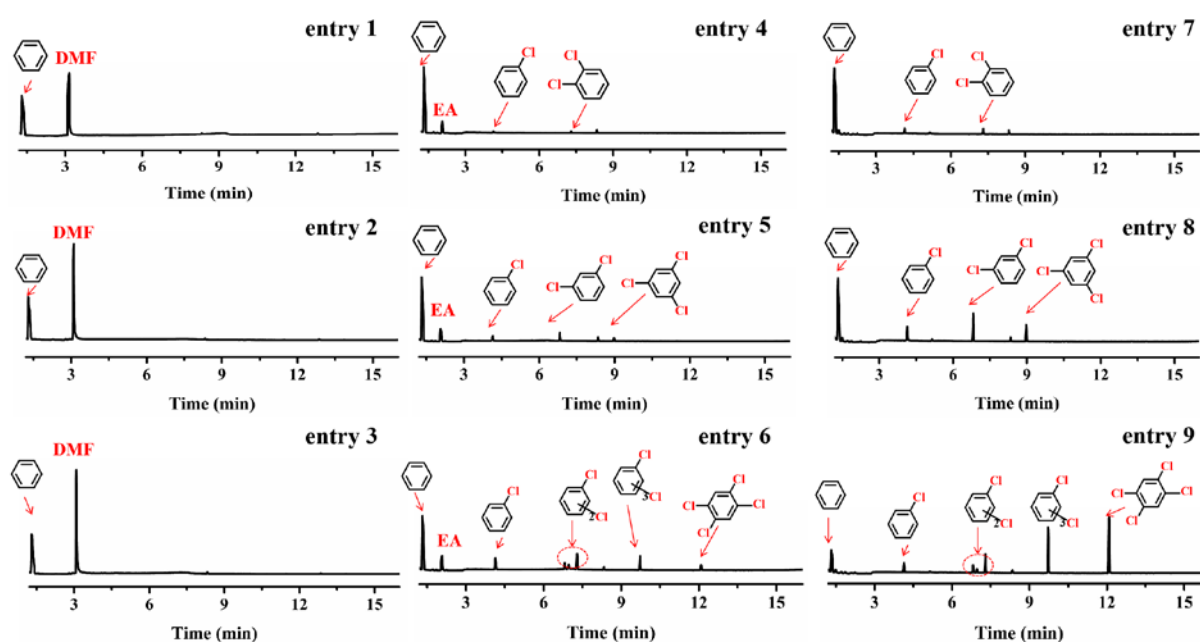

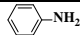

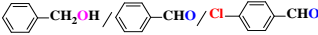

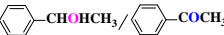
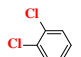
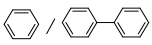
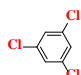
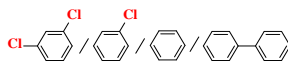
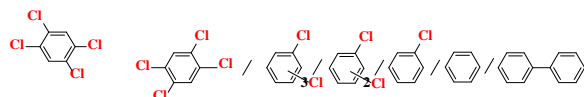


Figure S17. Gas chromatography (GC) analysis of the dechlorination of the multiple chlorinated substrates in a mixed solvent system in Table S4.

Table S5. Pd/C catalyzed dechlorination reaction.

Entry	Substrate	Product	T (h)	Conversion (%)	Carbon balance (%)
1			6	99	99
2			3	21/10/64	95
3			22	53/46	99
4			10	94/4	98
5			10	5/2/81/12	97



Reaction conditions: chlorinated substrate (0.05 mmol), catalyst (calculating according to 5 mol% of Pd), ammonium formate (1 mmol) and methanol (4 ml) at room temperature. A mixed solvent of methanol and N, N-dimethyl formamide (V/V, 1:1) was used in entry 4-6 because of the solubility concern. Conversion determined by GC-MS.

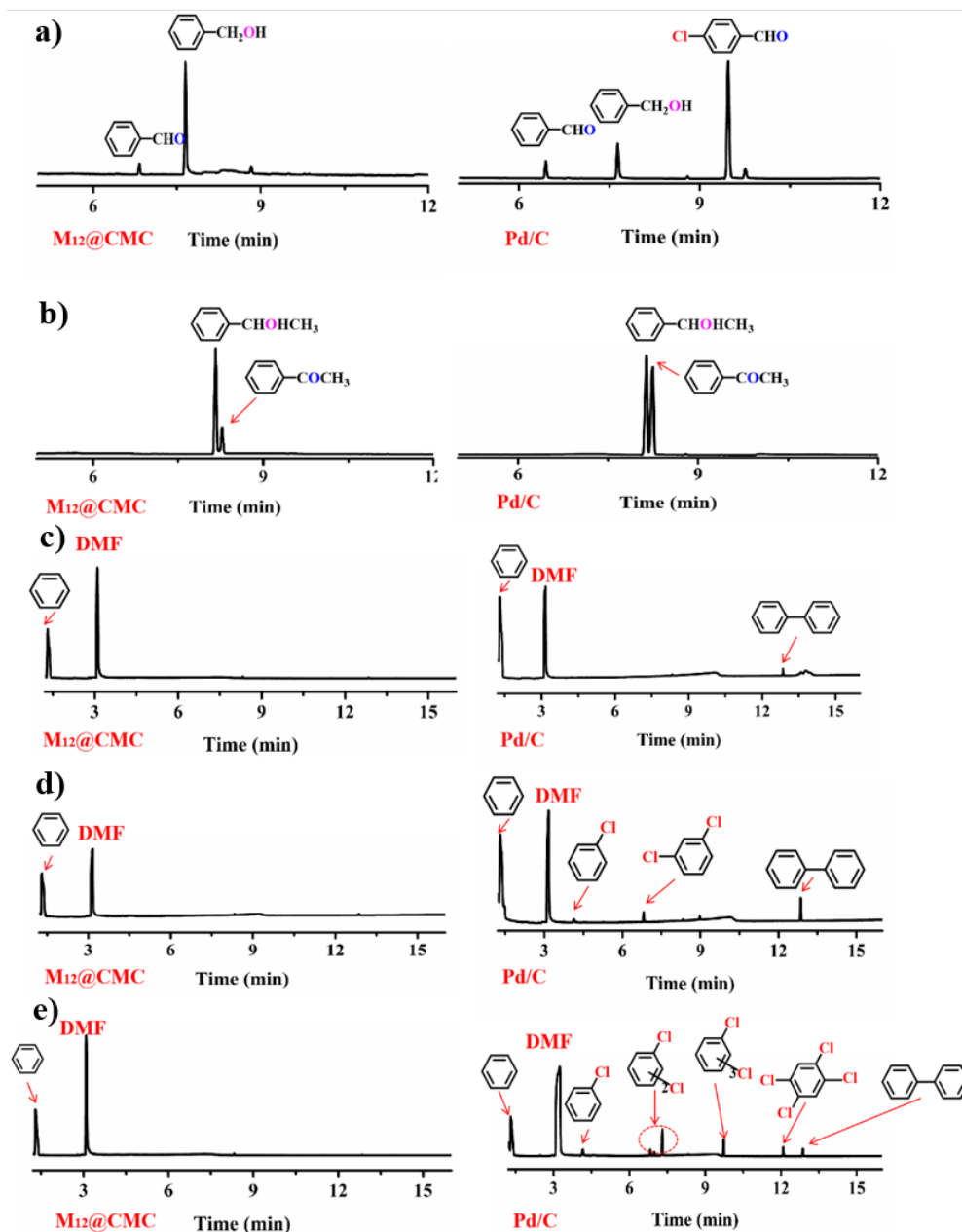


Figure S18. Gas chromatography (GC) analysis of the dechlorination reaction of 4-chlorobenzaldehyde (a), 4'-chloroacetophenone (b), 1,2-dichlorobenzene (c), 1,3,5-trichlorobenzene (d) and 1,2,4,5-tetrachlorobenzene (e) with the catalyst of **M₁₂@CMC** (left) and commercial Pd/C (right).

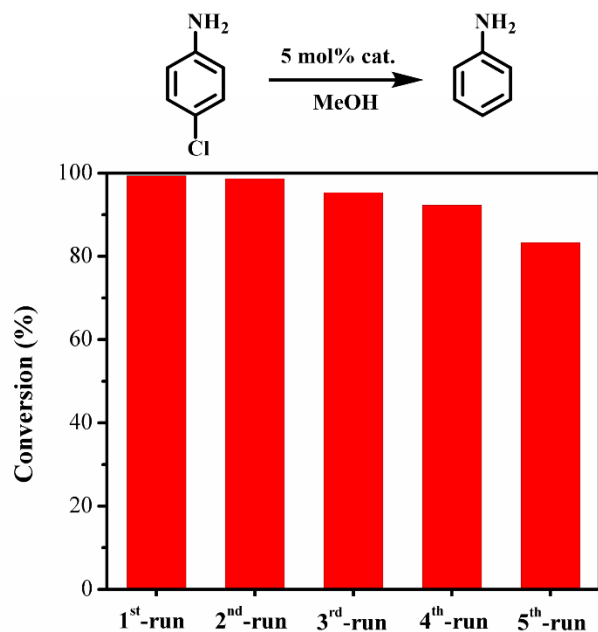


Figure S19. Recyclability experiments of $M_{12}@CMC$ in the dechlorination reaction. After each run, the catalyst was collected by filtration, washed by methanol, and dried for the next catalytic run under the same conditions. Note: ammonium formate serving as hydrogen source needs to be replenished in each catalytic run.

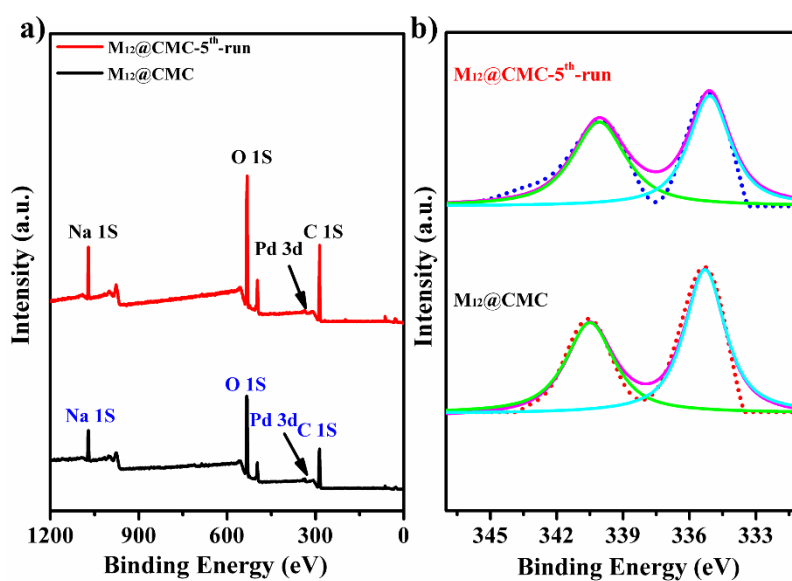


Figure S20. XPS spectra of $M_{12}@CMC$ before and after five cycles of reaction.: (i) survey spectra, (ii) high-resolution signals of Pd 3d.

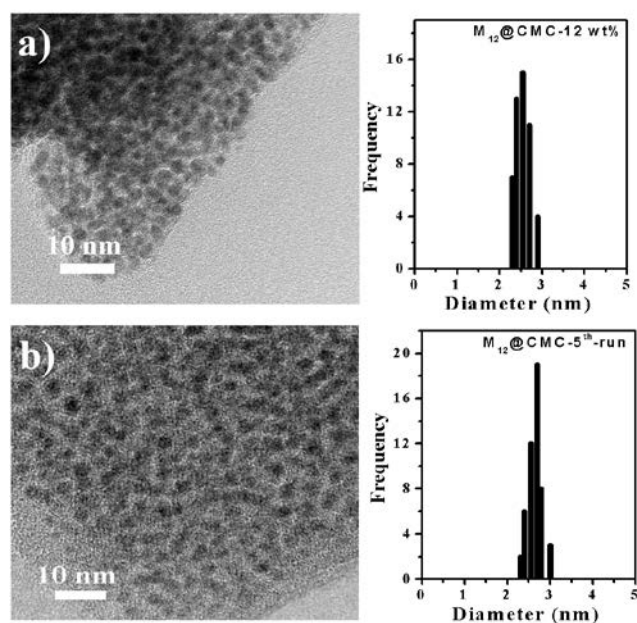


Figure S21. TEM images and histograms of size distributions of aerogels of $M_{12}@CMC$ (a) before and (b) after five cycles of reaction.

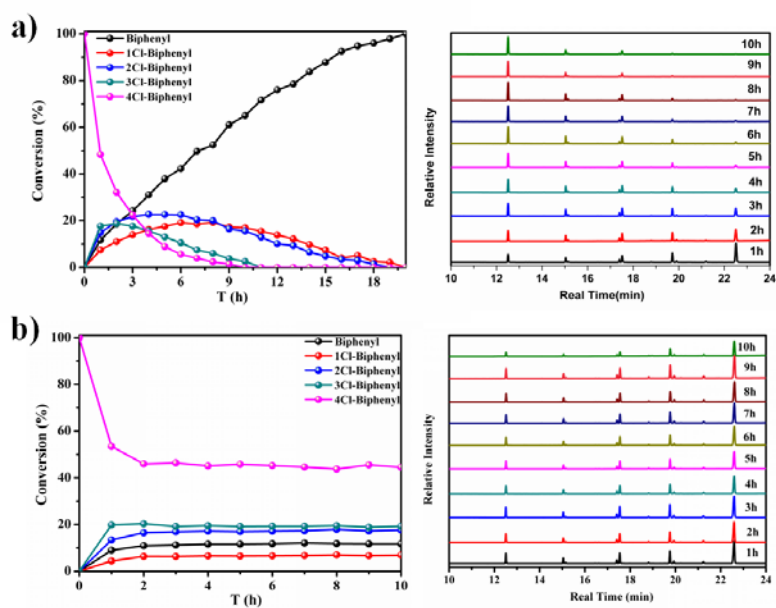


Figure S22. Degradation plot of PCB 77 with the catalyst of $M_{12}@CMC$ (a) and Pd/C (b) in MeOH/DMF in the stirred vessel. The conversion was determined by the in-situ recording of

the gas chromatography (GC) analysis. Chromatograms of tetrachlorinated biphenyls (22.58/21.3 min), trichlorinated biphenyls (20.0/19.7/18.8 min), dichlorinated biphenyls (17.6/17.5 min), chlorinated biphenyls (15.2/15.05 min) and biphenyl (12.5 min) in this process were indicated.



Figure S23. The image of the continuous-flow setup for PCB 77 degradation.

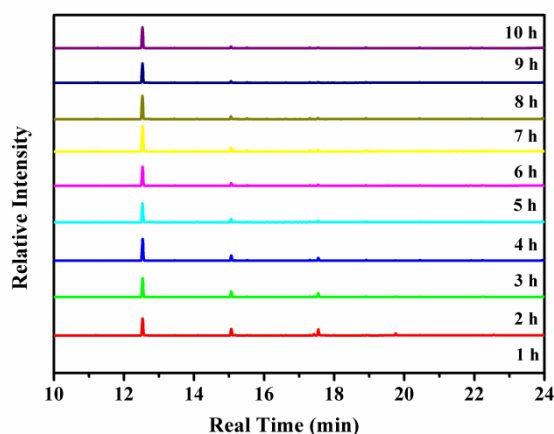


Figure S24. Gas chromatography (GC) analysis of the reaction solution of continuous flow-through operation for dechlorination reaction of 3,3',4,4'-tetrachlorobiphenyl, indicating the progress of dechlorination of different numbers of chlorine atoms in MeOH/DMF. Chromatograms of tetrachlorinated biphenyls (22.58/21.3 min), trichlorinated biphenyls (20.0/19.7/18.8 min), dichlorinated biphenyls (17.6/17.5 min), chlorinated biphenyls (15.2/15.05 min) and biphenyl (12.5 min) in this process were recorded.

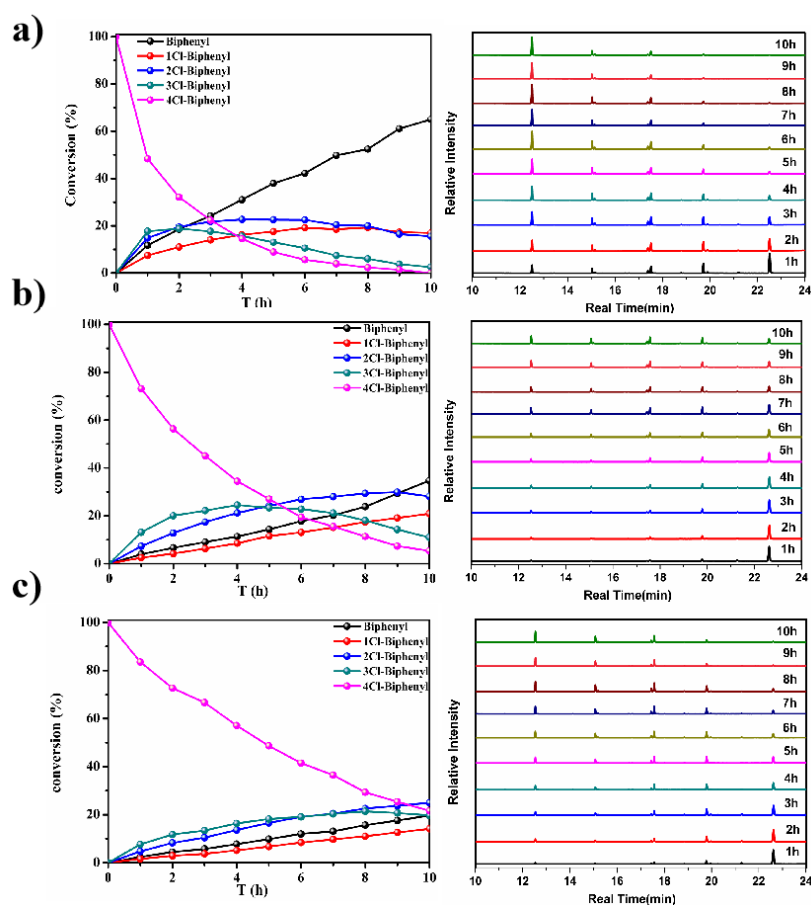


Figure S25. Degradation plot of PCB 77 with the catalyst of $M_{12}@CMC$ in a mixed solvent systems of methanol/N, N-dimethyl formamide (a), methanol/tetrahydrofuran (b), and methanol/ethyl acetate (c) in the stirred vessel. The conversion was determined by the in-situ recording of the gas chromatography (GC) analysis.

References

- S1. C. Desmarests, I. Azcarate, G. Gontard and H. Amouri, *Eur. J. Inorg. Chem.*, 2011, 4558.
- S2. F. Jiang, N. Wang, Z.-K. Du, J. Wang, Z.-G. Lan and R.-Q. Yang, *Chem. Asian J.*, 2012, **7**, 2230.
- S3. C. Li, Z.-Y. Gu, C. Zhang, S.-H. Li, L. Zhang, G.-Q. Zhou, S.-X. Wang and J.-C. Zhang, *European Journal of Medicinal Chemistry*, 2018, **144**, 662.
- S4. S. Wimmer, P. Castan, F. L. Wimmer and N. P. Johnson, *J. Chem. Soc., Dalton Trans.*, 1989, **403**.

S5. L.-X. Cai, S.-C. Li, D. N. Yan, L. P. Zhou, F. Guo and Q.-F. Sun, *J. Am. Chem. Soc.*, 2018, **140**, 4869.

S6. M. Fujita, D. Oguro, M. Miyazawa, H. Oka, K. Yamaguchi and K. Ogura, *Nature*, 1995, **378**, 469.